Mass Center Estimation in Spinning Drag-Free Satellites

J. DAVID POWELL*
Stanford University, Stanford, Calif.

In spinning drag-free satellites, mass center offsets on the order of millimeters will cause propellant consumption due to mass center motion to be the dominant factor in satellite lifetimes. Precise control of the mass center location in the design and fabrication of the satellite to make its effect negligible is difficult and expensive to achieve; however, by continually estimating the mass center location and controlling the satellite to spin about this point, propellant wastage attributable to the mass center location is eliminated. The design and laboratory construction of an analog mass center estimator is the subject of this paper. Analytical predictions of estimator accuracy were verified in the laboratory and it is concluded that the accuracy of this mechanization is approximately 25 μm (0.001 in.).

Introduction

THE drag-free satellite has a proof mass in an internal cavity and is controlled in translation so that the proof mass never touches the cavity walls. The proof mass is, therefore, in free fall primarily under the influence of gravitational forces because it is shielded from external forces, such as aerodynamic drag and solar pressure. The entire satellite is controlled to follow the proof mass and, therefore, is in a drag-free orbit.

The largest of the perturbing nongravitational forces which act on the proof mass are satellite mass attraction and proof mass position sensor forces. Because these forces are fixed to the satellite, spinning the satellite averages the forces in directions perpendicular to the spin vector. Lange[1] showed that perturbing forces acting in the intrack orbital direction cause much larger drag-free trajectory errors than any other direction; therefore, spinning the satellite with its spin vector normal to the orbital intrack direction substantially reduces the effect of perturbing forces.

In spinning drag-free satellites, mass center misalignments on the order of millimeters could cause substantial propellant consumption. In satellites weighing in the neighborhood of 100 kg, determining the mass center location and maintaining that location through the life of the satellite to this accuracy is a difficult and expensive proposition. In addition, stability of the proof mass position sensor null point to this accuracy is difficult to achieve. By estimating the mass center location and controlling to it, only the accuracy of the estimate need be on the order of tenths of millimeters; the only requirement on the mass center being that the proof mass not touch the cavity walls during control system operation.

Recently, much has been written on state estimation for linear systems. Summaries of stochastic-filter theory, including the Kalman and Wiener filters, can be found in the texts by Lee[2] and Deutsch.[3] Given the system equations and stochastic properties of the input and output noise, this theory yields an optimal solution for the filter-gain matrix. Schmidt[4] reviews and presents new ideas in compensating the stochastic optimal-filter gains for better estimation in the presence of modeling and mechanization errors. A technique for the construction of state estimators for noise-free systems was presented by Luenberger[5,6] and discussed by Gopinath[7] who described an intuitively appealing design method for minimal dynamic-order estimators. Many authors[5-9] consider the problem of determining the estimator gains, given the desired response characteristics (root locations) of the estimators. Luenberger[6] briefly discusses the bounds on the root locations; however, the author knows of no previous work that offers any insight into the selection of root locations for the noise-free case. This paper presents practical design considerations of an analog state estimator for this application. In particular, it discusses the influence of error sources such as deterministic modeling errors, component tolerances, and amplifier biases on the root locations, state vector definition, and dynamic order.

Control Problem

Equations of Motion

The equations of motion of the proof mass with respect to a reference frame fixed to the rotating satellite were given by Lange.[1] It is assumed in the equations used in this analysis that the satellite mass center position is stationary and that $\dot{\omega}_s = 0$. The latter assumption implies that the satellite is spinning about a principal axis, stably oriented with respect to the orbit plane, and that disturbing torques are negligible.[10] In this case, the equations of motion in the plane of spin coordinatized in a reference frame fixed to the satellite, and centered at the proof mass position sensor null point are

$$\begin{aligned} \ddot{x}_b - \omega_s^2 x_b - 2\omega_s \dot{y}_b &= f_{ix} + f_{bx} + f_{cx} - \omega_s^2 x_e \\ \ddot{y}_b - \omega_s^2 y_b + 2\omega_s \dot{x}_b &= f_{iy} + f_{by} + f_{cy} - \omega_s^2 y_e \end{aligned} \quad (1)$$

where x_b, y_b = position coordinates of the proof mass in the plane of spin with respect to the satellite, ω_s = satellite angular velocity, f_{ix}, f_{iy} = disturbing specific force acting on satellite (constant in nonrotating reference frame), f_{bx}, f_{by} = disturbing specific force acting on satellite (constant in rotating reference frame), f_{cx}, f_{cy} = control specific force on the satellite, x_e, y_e = mass center position coordinates.

Controller Equations

A linear controller was devised by Lange[1] for this system. Using his control law, a constant mass center displacement with no disturbing forces results in a constant control force. Physically, this control force provides the centripetal acceleration necessary to maintain the center of mass in a circular trajectory about the proof mass.

Presented as Paper 71-947 at the AIAA Guidance, Control and Flight Mechanics Conference, Hofstra University, Hempstead, N.Y., August 16–18, 1971; submitted October 14, 1971, revision received January 14, 1972. This research was supported by NASA under Contract NSR-05-020-379 and Research Grant NGR-05-020-019 and by the United States Air Force under Contract F33615-70-C-1637. The author wishes to acknowledge the help and interest of B. O. Lange and D. B. DeBra.

Index categories: Unmanned Earth Satellite Systems; Spacecraft Navigation, Guidance, and Flight Path Control; Spacecraft and Component Ground Testing and Simulation.

* Assistant Professor of Aeronautics and Astronautics. Member AIAA.

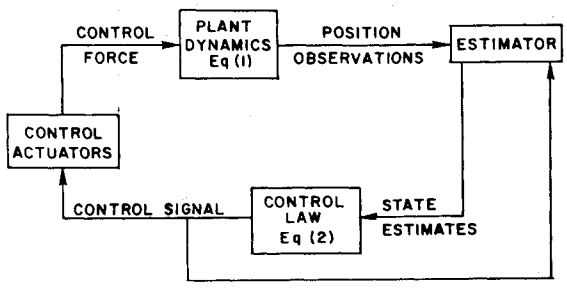

Fig. 1 System block diagram.

A constant external force with respect to a nonrotating reference frame (solar pressure for example) causes sinusoidal f_{ix}, f_{iy}. This disturbance produces a sinusoidal steady-state error in x_b, y_b.

If the magnitudes of the disturbing accelerations are available for use, it is possible to synthesize a better control law. A control law effectively using knowledge of disturbing forces is

$$f_{cx} = -k_p\{x_b - x_e' + \gamma[\dot{x}_b - \omega_s(y_b - y_e')]\} - f_{ix}$$
$$f_{cy} = -k_p\{y_b - y_e' + \gamma[\dot{y}_b + \omega_s(x_b - x_e')]\} - f_{iy} \quad (2)$$

where k_p = position gain
γ = velocity gain/position gain
$x_e' = x_e - f_{bx}/\omega_s^2$, $y_e' = y_e - f_{by}/\omega_s^2$ } "apparent center of mass"

The following two additions to Lange's control law have been made: 1) the control center has been shifted to the apparent center of mass (x_e', y_e') and 2) the external disturbing acceleration has been added. These additions yield the following benefits: 1) control effort caused by body-fixed forces and center-of-mass mis-alignment is eliminated at the expense of a shift in the steady-state values of x_b and y_b, and 2) No steady-state error occurs in x_b, y_b due to external forces; control effort is unchanged.

The laboratory simulator uses on-off, pulse-modulated control actuators and has a deadspace in the control law. The characteristics of these nonlinear control laws is analyzed in Ref. (11). This paper describes the design and construction of an estimator providing position, velocity, and mass center information for use in a control law similar to Eq. (2).

Estimator Design

The observations directly available are the proof mass position coordinates. The desired additional information, velocities and mass center location, is obtained by the estimator by processing the position observations and the control force signals. Figure 1 shows the role of the estimator in the control system block diagram.

The estimator design discussed is particularly directed toward continuous (or analog) mechanizations. This arbitrary choice was influenced by its simplicity in this application and by the fact that the observations are continuous.

Statement of the Estimation Equations

Luenberger[5,6] has shown that the state of a linear system can be estimated by the construction of a similar linear system driven by the available outputs and inputs of the system being observed. If the system to be observed is assumed to be described by

$$\dot{x} = Fx + Gu$$
$$y = Hx \quad (3)$$

where

$x = n \times 1$ state vector
$F =$ constant $n \times n$ system matrix
$G =$ constant $n \times m$ input matrix
$y = p \times 1$ output vector
$H =$ constant $p \times n$ output matrix
$u = m \times 1$ input vector

then an "estimator" or "observer" of the entire state vector of the system is given by

$$\dot{\hat{x}} = \bar{F}\hat{x} + \bar{G}u + L(y - \bar{H}\hat{x}) \quad (4)$$

where ($\hat{}$) denotes an estimated value, ($^-$) denotes the estimator mechanization of a physical quantity, $L =$ constant $n \times p$ estimator gain matrix. A state estimator for only the unavailable states (minimal-order observer) was also described by Luenberger. The measurements themselves are used along with the estimates to obtain complete state information.

The estimator design problem involves selecting an appropriate system description [Eqs. (3)], selecting the gain matrix L, choosing between the full-order observer [Eq. (4)] and the minimal-order observer, and specifying details of the mechanization. The aim of the following sections is to determine the effect of these choices on estimation accuracy and system complexity; the end goal is a balance between the two considerations.

Estimation-Equation Adaptation by State Augmentation

For the spinning drag-free satellite control problem (and laboratory simulation), a possible system description is given in Eq. (1). The states x_b and y_b (the position of the proof mass with respect to the sensor null) are directly available. The only terms of the input that are known are the control components f_{cx}, f_{cy}; however, the remaining terms can be modeled, augmented to the state vector, and their values estimated along with the other states. A reasonable model for the unknowns is 1) body-fixed disturbing accelerations: constant, 2) center-of-mass location: constant, and 3) "inertially" fixed disturbing accelerations (constant in a nonrotating reference frame): sinusoidal.

It is intuitively clear that, because body-fixed forces and center-of-mass offsets have been modeled to look like constant inputs to the system, it will be impossible to obtain separate estimates of these quantities. This can be verified mathematically by postulating separate states for these quantities and by checking the observability[3] of the resulting system. When assuming knowledge of these terms, however, the control law [Eqs. (2)] did not require separate estimates of the states; its only requirement was for the apparent center of mass which was defined to be

$$x_e' = x_e - f_{bx}/\omega_s^2; \quad y_e' = y_e - f_{by}/\omega_s^2$$

Augmenting the state vector with this combined term does satisfy the observability requirement, and system equations for use in constructing the estimator are

$$\begin{bmatrix} \dot{x}_b \\ \dot{y}_b \\ \dot{u}_b \\ \dot{v}_b \\ \dot{x}_e' \\ \dot{y}_e' \\ \dot{f}_{ix} \\ \dot{f}_{iy} \end{bmatrix} = \left[\begin{array}{cc|cccccc} 0 & 0 & 1 & 0 & 0 & 0 & 0 & 0 \\ 0 & 0 & 0 & 1 & 0 & 0 & 0 & 0 \\ \hline \omega_s^2 & 0 & 0 & 2\omega_s & -\omega_s^2 & 0 & 1 & 0 \\ 0 & \omega_s^2 & -2\omega_s & 0 & 0 & -\omega_s^2 & 0 & 1 \\ 0 & 0 & 0 & 0 & 0 & 0 & 0 & 0 \\ 0 & 0 & 0 & 0 & 0 & 0 & 0 & 0 \\ 0 & 0 & 0 & 0 & 0 & 0 & 0 & \omega_s \\ 0 & 0 & 0 & 0 & 0 & 0 & -\omega_s & 0 \end{array}\right] \begin{bmatrix} x_b \\ y_b \\ u_b \\ v_b \\ x_e' \\ y_e' \\ f_{ix} \\ f_{iy} \end{bmatrix} + \left[\begin{array}{cc} 0 & 0 \\ 0 & 0 \\ \hline 1 & 0 \\ 0 & 1 \\ 0 & 0 \\ 0 & 0 \\ 0 & 0 \\ 0 & 0 \end{array}\right] \begin{bmatrix} f_{cx} \\ f_{cy} \end{bmatrix} \quad (5)$$

where $u_b = \dot{x}_b$, $v_b = \dot{y}_b$, and the states x_b, y_b are directly observed.

Design Considerations

For this application, the design of an estimator is an iterative process between the considerations contained in the following sections. Design variables are evaluated typically by their effect on estimation accuracy; hence, the estimator-error equations are developed first.

Error equations

Figures 2a and 2b are two different configurations of the full-order observer given by Eq. (4). Error sources considered are a) amplifier biases (b_i and b_s in Fig. 2), b) mechanization errors of physical quantities (G, F), c) mismatch of L mechanization in two locations (Fig. 2b), d) nonmodeled inputs, e) observation scaling errors, and f) observation noise.

Equations (3) and (4) are restated to include error sources: Dynamical system:

$$\dot{x} = Fx + Gu + G_n u_n$$
$$y = (I + \delta_s)Hx + q \tag{6}$$

where $G_n = n \times l$ distribution matrix for nonmodeled inputs, $u_n = l \times 1$ nonmodeled input vector, $\delta_s = p \times p$ diagonal scaling-error matrix, $q = p \times 1$ noise vector.

$$\begin{bmatrix} \dot{x}_b \\ \dot{y}_b \\ \dot{u}_b \\ \dot{v}_b \\ \dot{x}_e' \\ \dot{y}_e' \end{bmatrix} = \left[\begin{array}{cc|cccc} 0 & 0 & 1 & 0 & 0 & 0 \\ 0 & 0 & 0 & 1 & 0 & 0 \\ \hline \omega_s^2 & 0 & 0 & 2\omega_s & -\omega_s^2 & 0 \\ 0 & \omega_s^2 & -2\omega_s & 0 & 0 & -\omega_s^2 \\ 0 & 0 & 0 & 0 & 0 & 0 \\ 0 & 0 & 0 & 0 & 0 & 0 \end{array}\right] \begin{bmatrix} x_b \\ y_b \\ u_b \\ v_b \\ x_e' \\ y_e' \end{bmatrix} + \begin{bmatrix} 0 & 0 \\ 0 & 0 \\ 1 & 0 \\ 0 & 1 \\ 0 & 0 \\ 0 & 0 \end{bmatrix} \begin{bmatrix} f_{cx} \\ f_{cy} \end{bmatrix} \tag{11}$$

Estimator A (Fig. 2a)

$$\dot{\hat{x}} = \bar{F}x + L(b_s + y - H\hat{x}) + \bar{G}u + b_i \tag{7}$$

Estimator B (Fig. 2b)

$$\dot{\hat{x}} = (\bar{F} - L\bar{H})\hat{x} + (L + \delta L)y + \bar{G}u + b_i \tag{8}$$

where $b_i = n \times 1$ integrator bias vector, $b_s = p \times 1$ summing-amplifier bias vector, $\delta L = n \times p$ matrix of the difference between L in the two locations.

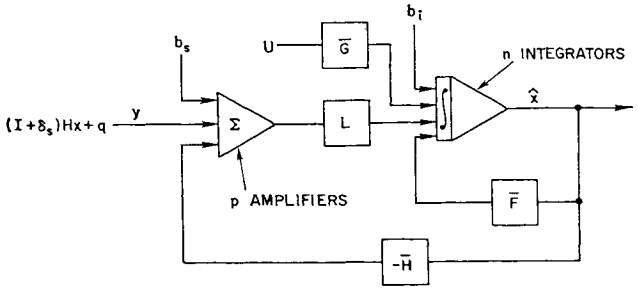

a) Full-order estimator with summation amplifiers, Eq. (4).

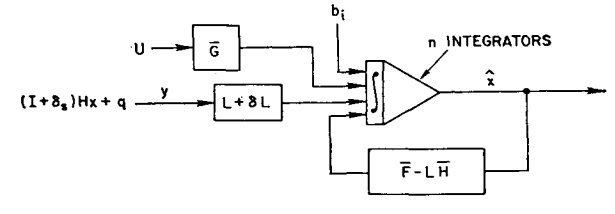

b) Full-order estimator without summation amplifiers, Eq. (4).

Fig. 2 Estimator mechanizations.

The error equations for the above mechanizations are obtained by subtracting the estimator equations from the dynamical-system equations and are, to first order:
Estimator A—error equation

$$\dot{\varepsilon} = [F + \delta_F - LH]\varepsilon - \delta_F x - \delta_G u + G_n u_n - L\delta_s Hx - Lq - Lb_s - b_i + L\delta_H x \tag{9}$$

where $\varepsilon = x - \hat{x}$, $\delta_F = \bar{F} - F$, $\delta_G = \bar{G} - G$, $\delta_H = \bar{H} - H$.
Estimator B—error equation

$$\dot{\varepsilon} = [F + \delta_F - LH]\varepsilon - \delta_F x - \delta_G u + G_n u_n - L\delta_s Hx - Lq - Lb_s - b_i + L\delta_H x - \delta_L Hx \tag{10}$$

Dynamic model

A dynamic model of the system is given in Eq. (5). A particular state-vector definition has been assumed; however, the dynamic model is invariant for any linear transformation of the representations. This section discusses the consequences of assumptions pertaining to the dynamics, and the following section discusses the consequences of the particular state-vector definition used to represent the model.

For this problem, the only required state estimates are position, velocity and mass center; hence, neglecting the inertial disturbing forces will yield a simpler model if the estimation errors caused by the omission are acceptable. In this case, the estimation model is

and the nonmodeled inertial force is an error source to the estimation process.

The estimation error caused by this perturbing input is described by

$$\dot{\varepsilon} = [F - LH]\,\varepsilon + f_i \begin{bmatrix} 0 \\ 0 \\ \cos \omega_s t \\ -\sin \omega_s t \\ 0 \\ 0 \end{bmatrix} \tag{12}$$

where f_i is the magnitude of the specific inertial force. This error is dependent on the estimator roots [or eigenvalues of $(F - LH)$] as well as on f_i and, therefore, the effect of this error source is considered in the selection of L. If it had not been possible to select values of L that sufficiently attenuated the effect of this error source, the more complex dynamic model, including an estimate of inertial forces, would be required.

State-variable selection

It is well-known that if a model of a system is given by

$$\dot{x} = Fx + Gu$$

a state estimator can be constructed using a state-vector definition which is any linear combination of x. Reasons for selecting any one state-vector definition over any other are a) to reduce estimation errors and b) to make certain quantities directly available for display or use in the controller. A goal of the estimator/controller mechanization in the laboratory simulator was to verify the capability to estimate the center-of-mass of the simulator and to control to this estimate.

The control law for this system is [see Eqs. (2)]

$$e_x' = x_b - x_e' + \gamma[u_b - \omega_s(y_b - y_e')]$$
$$e_y' = y_b - y_e' + \gamma[v_b + \omega_s(x_b - x_e')] \quad (13)$$

therefore, selection of e_x', e_y' as two of the states eliminates any need for summation amplifiers to form the control law. Because x_e' and y_e' were desired for display, they were also selected as states. To complete the state definition for the Eq. (11) model, the two remaining states were selected to be

$$\mathscr{X} = x_b - x_e'$$
$$\mathscr{Y} = y_b - y_e' \quad (14)$$

It will be seen that this choice provides a reduction in estimation errors over the state definition shown in Eq. (11) for the same model. The system representation with this state definition is

$$\begin{bmatrix} \dot{\mathscr{X}} \\ \dot{\mathscr{Y}} \\ \dot{e}_x' \\ \dot{e}_y' \\ \dot{x}_e' \\ \dot{y}_e' \end{bmatrix} = \begin{bmatrix} -1/\gamma & \omega_s & 1/\gamma & 0 & 0 & 0 \\ -\omega_s & -1/\gamma & 0 & 1/\gamma & 0 & 0 \\ -1/\gamma & 0 & 1/\gamma & \omega_s & 0 & 0 \\ 0 & -1/\gamma & -\omega_s & 1/\gamma & 0 & 0 \\ 0 & 0 & 0 & 0 & 0 & 0 \\ 0 & 0 & 0 & 0 & 0 & 0 \end{bmatrix} \begin{bmatrix} \mathscr{X} \\ \mathscr{Y} \\ e_x' \\ e_y' \\ x_e' \\ y_e' \end{bmatrix} + \begin{bmatrix} 0 & 0 \\ 0 & 0 \\ 1 & 0 \\ 0 & 1 \\ 0 & 0 \\ 0 & 0 \end{bmatrix} \begin{bmatrix} f_{cx} \\ f_{cy} \end{bmatrix} \quad (15a)$$

and

$$\begin{bmatrix} x_m \\ y_m \end{bmatrix} = \begin{bmatrix} 1 & 0 & 0 & 0 & 1 & 0 \\ 0 & 1 & 0 & 0 & 0 & 1 \end{bmatrix} \begin{bmatrix} \mathscr{X} \\ \cdot \\ \cdot \\ \cdot \\ \cdot \end{bmatrix} \quad (15b)$$

where x_m, y_m are the measured values of x_b and y_b.

For a linear controller without inertial disturbing forces, the equilibrium values of the states of Eq. (15a) are all zero except x_e', y_e', whereas for the state definition in Eq. (11), the equilibrium values of x_b, y_b are x_e', y_e'. These equilibrium states, coupled with the fact that the right-hand two columns of F (and, therefore, δ_F) are zero for the Eqs. (15) model, show that the error-equation input term for Eqs. (15) is always zero but is proportional to the center-of-mass location for the Eq. (11) system representation. No other choice of states in place of ($\mathscr{X}$, $\mathscr{Y}$) has this property.

Gain-matrix selection

Assuming that the desired estimator root locations are known, algorithms for the computation of the gain matrix (L), involving transformations of the system equations to various canonical forms, have been devised.[6,8,9] For many multioutput systems, no unique L exists for a given set of root locations. This freedom is exploited by Gopinath[7] by restricting L to a certain form which then greatly simplifies the algorithm. The arbitrariness in the design is resolved by the other authors, in these cases, by the transformation of the system equations to a particular canonical form.

In this application, it was decided that choosing a form of L, which simplified the estimator mechanization, made better use of the design freedom than one that simplified the calculations. The characteristics of L chosen are a) symmetry between x and y axes and b) no cross-coupling, which means that regardless of the state definition, L is of the form

$$\begin{bmatrix} L_1 & 0 \\ 0 & L_1 \\ \hline L_2 & 0 \\ 0 & L_2 \\ \hline L_3 & 0 \\ 0 & L_3 \end{bmatrix} \quad (16)$$

where the equal diagonals in each 2×2 submatrix implies symmetry, and the zeros on the off diagonals eliminate cross-coupling. The symmetry assumption is a natural one because both axes of the estimator are identical. The omission of cross-coupling terms is not justified so easily; in fact, in some cases, this omission may make desirable root locations inaccessible. In this application, the freedom available in the selection of root locations was sufficient for a good estimator design. Cross-coupling exists in the plant dynamics and is retained in the estimator model of those dynamics.

The practical advantages of this L form are as follows: a) design of one axis of the estimator is identical to the other, b) cross-coupling between the axes is kept to a minimum, which results in fewer components, and c) modification of the estimator for use with a nonrotating simulator is simplified. Use of this form, however, rules out any of the techniques referenced above for computing the components of L, given the desired root locations. This difficulty was resolved by selecting the components of L directly subject to the restriction that the resulting roots are well damped. Given values of L, the damping of the resulting roots is easily determined using standard computerized linear-system analysis techniques such

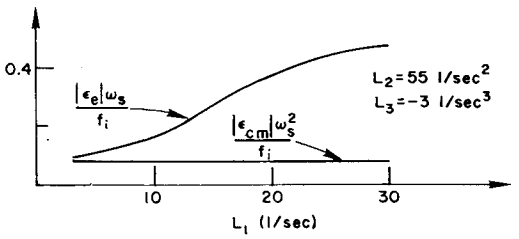

a) Estimation error vs L_1.

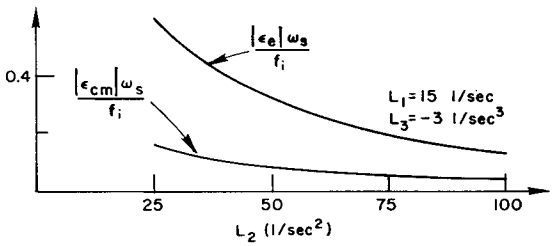

b) Estimation error vs L_2.

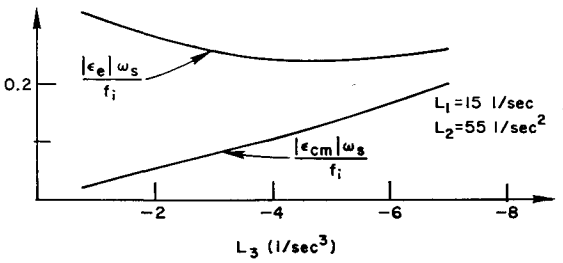

c) Estimation error vs L_3.

Fig. 3 Estimation errors vs gain-matrix values.

as *The General Stability Analysis Program*.[12] Because the damping restriction does not uniquely define the components of L, the effect on the estimation errors was judged to be the appropriate criterion for the selection of the remaining degree of freedom in the gain matrix.

For the drag-free satellite simulator with a system model given by Eqs. (15) and estimator mechanization A in Fig. 2, the dominant estimation errors are caused by the nonmodeled input f_i. The influence of the L components on the estimation error is shown in Fig. 3. These results, coupled with the effect of L on root locations, provided the necessary information to select the gain matrix. The selected design values

$$L_1 = 15 \text{ sec}^{-1}$$
$$L_2 = 55 \text{ sec}^{-2}$$
$$L_3 = -3 \text{ sec}^{-3}$$

represent a hardware upper limit on L_2, a value of L_1 yielding well damped roots given L_2, and a value of L_3 judged to produce acceptable center-of-mass estimate errors in the presence of typical inertial disturbing forces. If it had not been possible to obtain acceptable center-of-mass estimate errors, use of the more complex dynamic model, which removes this error source (see section on dynamic modeling), would allow use of other criteria in selecting L, thereby reducing errors caused by other sources, as well as eliminating errors due to f_i.

The hardware limitation is a function of the output impedance of the particular integrated-circuit operational amplifiers used in the construction of the estimator. If sufficient motivation for higher values of L_2 had existed, amplifiers with better performance could have been obtained. The upper limit on the design value of L_2, in the absence of hardware limitations, would be determined by estimation errors caused by noise or integrator biases.

Estimator order and mechanization

The algorithms are presented for two full-order estimator mechanizations in Eqs. (7) and (8). It is also possible to mechanize the estimator with a minimal-order estimator. The purpose of this section is to show that estimator A yields superior performance for this problem, with some increase in complexity. Table 1 illustrates the complexity differences by comparing amplifier requirements for the two dynamic models. Two observations are assumed.

The only difference between the error equations for estimators A and B is the additional term $\delta_L Hx$ in B; of consequence, is whether the effect of this term is significant, compared to all other error sources. Neglecting f_i, δ_L can be shown to be significant by assuming that the controlled system has reached steady state at its equilibrium point. In this condition, the estimation errors caused by all existing error sources except noise are constant and given by

$$\varepsilon = [F - LH]^{-1}(\delta_F x + L\delta_s Hx + Lb_s + b_i - L\delta_H x + \delta_L Hx) \tag{17}$$

and, for a system structured as in Eq. (11), the gain matrix L does not appear in $[F - LH)^{-1}L$, implying that estimation errors arising from δ_s, δ_H, and b_s are not affected by the choice of L. The errors caused by the remaining sources (δ_F, b_i, and δ_L), however, are affected by the values of L, and the relative importance of $\delta_L Hx$ is dependent, therefore, on L, F, and H, as well as on the values of the error sources. For the parameter values existing on the simulator (Ref. 10) and the L values given earlier, Eq. (17) reveals that elements of $\delta_L Hx$ typically cause estimation errors an order of magnitude or more greater than any other error source. This is true if $[F - LH]^{-1}$ does not depend on the value of L and if some elements of L are very large compared to the elements of F and H.

Table 1 Number of amplifiers required for estimator mechanizations

Dynamic model	No. of states	No. of amplifiers: Full order, Estimator A	Full order, Estimator B	Minimal order estimator
Eq. (11)	6	8	6	8
Eq. (5)	8	10	8	12

The minimal-order estimator contains the terms which are analogous to the offending term δ_L in estimator B. Under the large L assumption, these terms share the property that they represent the difference in mechanized values of large quantities that occur in more than one location in the estimator. Estimator A circumvented this problem by only requiring the mechanization of L in one location; therefore, the inability to mechanize the desired value of L in that location only results in differences in the root locations or transient response of the estimator. Because of the existence of these L mechanization error sources and no complexity advantage (Table 1), a minimal-order estimator was rejected for this application.

Conclusions

The design of an estimator for a specific application has been discussed, and the following observations have been made: 1) The choice of dynamic model need not represent all known dynamics of the system; furthermore, propagation of errors caused by omission of dynamic elements can be minimized by judicious selection of the gain matrix; 2) In a practical analog system with realistic sources of error, root locations have a large effect on the resulting estimation errors; 3) Reduction in estimation errors can be realized by proper selection of the state vector; however, the strongest influence on the state vector was the desire to have certain quantities directly available; and 4) In the class of problems where the elements of the gain matrix L are much larger than the elements of the system matrices F and H, and $[F - LH]^{-1}L$ is not dependent on the value of L, errors are significantly reduced by using estimator mechanization A in Fig. 2.

Experimental Verification

General Description

The experimental program, reported here, employed a laboratory simulation of the drag-free satellite translational-control system. The simulator has existed at Stanford University in various evolutionary forms since 1964. Figure 4 is a photograph of the laboratory apparatus. The simulator floats on an air film over a precisely level granite table[13] with negligible friction. The equations of motion of the orbital behavior [Eq. (1)] represent the relative motion between proof mass and satellite. In the laboratory, the proof mass is attached to the table and the simulator is free to move about it in the plane of the table. This duplicates the orbital equations of motion.

The simulator has spin-up gas jets that release compressed nitrogen providing an angular acceleration of the simulator. These jets are actuated by the operator through a model airplane radio transmitter. A smaller pair of spin maintenance jets provides a torque balancing air friction torques and maintains the simulator at a constant spin rate.

Data are available from the rotating simulator through a slip-ring/follower arm assembly[14] designed to provide negligible disturbing forces on the simulator. Photosensitive transistors on a follower arm detect the location of a light source on the vehicle and a servomotor controls the arm to follow the light source. Fine wires for the data running between the vehicle and the follower arm are under no tension, therefore transmit no force to the vehicle.

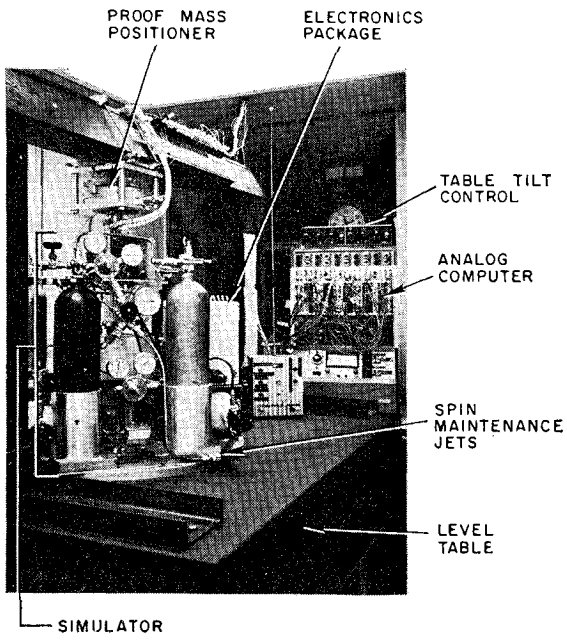

Fig. 4 Experimental apparatus.

Control-system description

The simulator control system consists of a proof-mass position sensor, compensation or state estimation, dead-space, modulator, and gas jets (Fig. 5).

The position sensor is a capacitive type which provides approximately linear output (x_m, y_m) vs proof-mass position (x_b, y_b) for approximately 0.050 in. of the 0.080 in. movement possible within the cavity. For a more detailed description see Ref. (15).

In the mechanization, ω_s is assumed to be -1 rad/sec in the spinning control law, γ was selected to be 1 (sec), and k_p/ω_s^2 can be varied $(0 < k_p/\omega_s^2 \lesssim 20)$ by adjusting the compressed-nitrogen pressure regulation. The system representation assumed for this mechanization is given in Eqs. (15) and yields the following estimation equations:

$$\begin{bmatrix} \dot{\hat{x}} \\ \dot{\hat{y}} \\ \dot{e}_x' \\ \dot{e}_y' \\ \dot{x}_e' \\ \dot{y}_e' \end{bmatrix} = \begin{bmatrix} -1/\gamma & \omega_s & 1/\gamma & 0 & 0 & 0 \\ -\omega_s & -1/\gamma & 0 & 1/\gamma & 0 & 0 \\ -1/\gamma & 0 & 1/\gamma & \omega_s & 0 & 0 \\ 0 & -1/\gamma & -\omega_s & 1/\gamma & 0 & 0 \\ 0 & 0 & 0 & 0 & 0 & 0 \\ 0 & 0 & 0 & 0 & 0 & 0 \end{bmatrix} \begin{bmatrix} \hat{x} \\ \hat{y} \\ \hat{e}_x' \\ \hat{e}_y' \\ \hat{x}_e' \\ \hat{y}_e' \end{bmatrix} + \begin{bmatrix} 0 \\ 0 \\ f_{cx} \\ f_{cy} \\ 0 \\ 0 \end{bmatrix} + \begin{bmatrix} L_1 & 0 \\ 0 & L_1 \\ L_2 & 0 \\ 0 & L_2 \\ L_3 & 0 \\ 0 & L_3 \end{bmatrix} \begin{bmatrix} x_m - \hat{x} - \hat{x}_e' \\ y_m - \hat{y} - \hat{y}_e' \end{bmatrix} \tag{18}$$

The estimator mechanization is basically a special-purpose analog computer. The four ω_s terms can be switched out for estimation while the simulator is not spinning, and the center-of-mass integrators (x_e' and y_e') can be shorted out for estimation of position and velocity states only. In the breadboard electronics, the estimator occupied two 4 × 6 in. cards.

The gas-jet modulator was selected so as to approximate a linear relationship between control force (f_{cx}, f_{cy}) and the error signal (e_x, e_y). The type mechanized is a pulse-width pulse-frequency (PWPF) scheme.

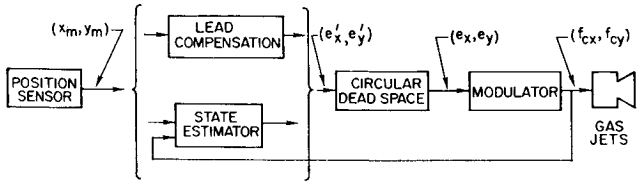

Fig. 5 Simulator control system.

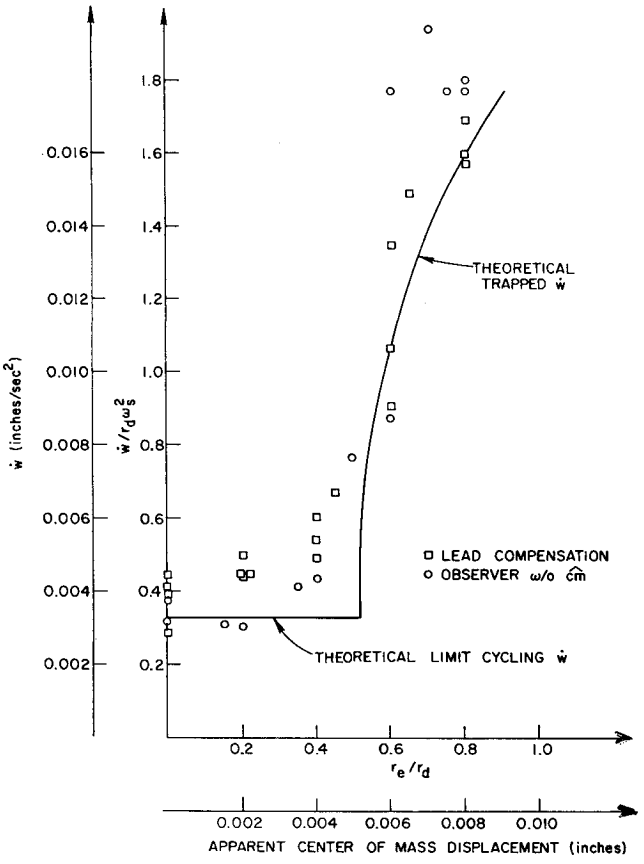

Fig. 6 Control effort vs apparent center of mass.

Estimation Accuracy

In the calibration of the estimator, the amplifier biases were nulled. This ensures that the estimator center-of-mass estimates read zero when all estimator inputs are zero. This static calibration is the only guarantee that the dc value of the estimates are the correct values of the apparent center of mass because no independent determination of the center of mass was available. However, in verifying a theory [called trapping,[10,11]] developed to predict control effort vs mass center location when mass center estimates are not used in the control law, estimates of the center of mass were employed to locate the data points. Figure 6 compares the experimental data

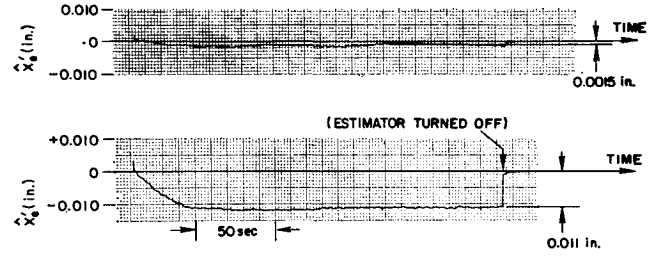

Fig. 7 Verification of analog-estimator mass center estimation accuracy.

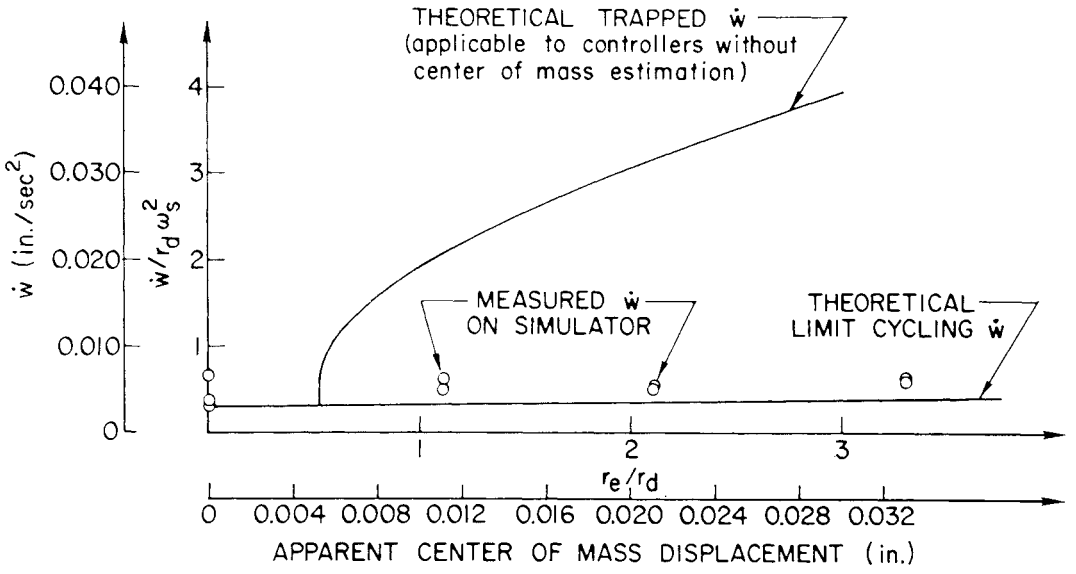

Fig. 8 Control effort vs apparent center of mass with center-of-mass estimation.

with theoretical predictions. Because these data show good agreement, it is assumed that both trapping theory and center-of-mass estimates are correct, rather than both being wrong with the errors canceling each other.

The preceding discussion pertains to the absolute accuracy of the center-of-mass estimates. Verification of the estimator's ability to measure changes in the center-of-mass location is much easier. Figure 7 shows the x_e' estimates before and after a 0.010 in. sensor-housing displacement. Because the simulator-to-sensor-housing weight ratio is approximately 20:1, this displacement results in a 0.0095 in. change in the center-of-mass location with respect to the sensor-null point. This change is verified in Fig. 7 within the ability to read the data, or ± 0.0005 in. Turning the estimator off near the end of each strip caused the step in the trace and provided a check on possible recorder null drift.

The fundamental reason for including a center-of-mass estimate in the simulator is to eliminate the high-control effort required to offset center-of-mass displacements and body-fixed forces. Figure 8 presents the experimental measurements of the control effort of the simulator while controlling to the center-of-mass estimate and verifies the substantial control-effort reduction realized by this type of control law when no inertial forces are present. Two curves are also shown; the lower represents the limit-cycling control effort and the upper represents the theoretical control effort of a system without center-of-mass estimation.

Conclusions

The design of an analog mass center estimator for a spinning drag-free satellite has been discussed and experimentally verified in the laboratory. In the design process, the goal was to achieve a balance between complexity and the minimization of the effect of the most significant error sources. It was demonstrated that root locations have a large effect on estimation errors as do the selection of other design variables. The selection of these variables is often considered to be an arbitrary choice in the literature. It was also concluded that a minimal-order estimator yields no reduction in complexity for this application and possesses characteristics that inherently cause larger estimation errors.

Analytical predictions of estimator accuracy were verified in the laboratory and it is concluded that the accuracy of this mechanization is approximately 25 μm (0.001 in.). Although the laboratory simulation does not duplicate all aspects of orbital designs, a 0.1 mm accuracy goal in an orbital mass center estimator appears quite feasible.

References

[1] Lange, B. O., "The Drag-Free Satellite," *AIAA Journal*, Vol. 2, No. 9, Sept. 1964, pp. 1590–1606.

[2] Lee, R. C. K., *Optimal Estimation, Identification, and Control*, Research Monograph No. 28, MIT Press, Cambridge, Mass., 1964.

[3] Deutsch, R., *Estimation Theory*, Prentice-Hall, Englewood Cliffs, N.J., 1965.

[4] Schmidt, S. F., "Compensation for Modeling Errors in Orbit Determination Problems," Rept. 67–16, Nov. 1967, Analytical Mechanics Associates, Palo Alto, Calif.

[5] Luenberger, D. G., "Observing the State of a Linear System," *IEEE Transactions on Military Electronics*, MIL-8, April 1964, pp. 75–80.

[6] Luenberger, D. G., "Observers of Multivariable Systems," *IEEE Transactions on Automatic Control*, AC-11, April 1966, pp. 190–197.

[7] Gopinath, B., "On the Identification and Control of Linear Systems," SUDAAR Rept. 351, June 1968, Stanford University, Stanford, Calif.

[8] Singer, R. A., "The Design and Synthesis of Linear Multivariable Systems with Application to State Estimation," SEL-68-030, June 1968, Stanford Electronics Labs, Stanford Univ., Stanford, Calif.

[9] Chen, R. T. N., "On the Construction of State Observers in Multivariable Control Systems," National Electronics Conference Inc., Dec. 8-10, 1969, Chicago, Ill.

[10] Powell, J. D. and Lange, B. O., "Control of a Spinning Drag-Free Satellite with an Application of Estimation Theory," SUDAAR Rept. 402, May 1970, Stanford Univ., Stanford, Calif.

[11] Powell, J. D., "Trapping—A Control Phenomenon of Spinning Drag-Free Satellites," IFAC Symposium on Automatic Control in Space, Dubrovnik, Yugoslavia, Sept. 6-10, 1971.

[12] Whitsmeer, A. J., "Preliminary Design Studies of Attitude-Control Systems for the Stanford Relativity Satellite," SUDAAR Rept. 337, Jan. 1968, Stanford Univ., Stanford, Calif.

[13] DeBra, D. B. et al, "A Precision, Active, Table-Leveling System," *Journal of Spacecraft and Rockets*, Vol. 5, No. 9, Sept. 1968, pp. 1040–1045.

[14] "Eighth Semiannual Status Report on the Engineering Portion of a Research Program to Develop a Zero-g Drag-Free Satellite and To Perform a Test of General Relativity," Nov. 1967, Dept. of Aeronautics and Astronautics, Stanford University, Stanford, Calif.

[15] Passy, Ury, "Simulation and Optimization Studies of the Drag-Free Satellite," SUDAAR Rept. 295, Nov. 1966, Stanford Univ., Stanford, Calif.